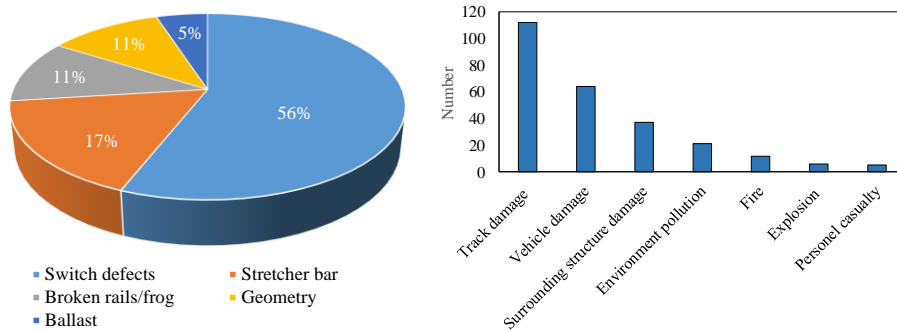


37 **1 Introduction**

38 The transportation of goods across the world heavily relies on rail freight transport. A
39 classification yard is used to separate railway vehicles onto one of several tracks. The railway turnout
40 (RT) is a vital element in a classification yard that guides trains from one track to another. Ensuring
41 train safety, especially at RTs in a classification yard, is currently facing significant challenges due to
42 increased transport demand, and the long-term service of the equipment [1, 2]. The derailments related
43 to infrastructure in the UK account for approximately 39% [3]. Over the past 15 years, maintenance
44 costs have constituted half of the total. By investigating the impact of infrastructure on derailments,
45 more than 50% of train derailments are caused by switch defects, as shown in Fig. 1 (a). In China,
46 where more than 250,000 turnouts are in use, there have been over 100 derailments at low-speed
47 turnouts in the past five years. Ensuring train safety and reducing secondary damage and injuries is the
48 primary goal of railway authorities. Although operators strictly adhere to safety standards and weather
49 conditions are not extreme, train derailments and corresponding damages can still occur at RTs due to
50 other factors such as track defects, poor alignments, as well as vehicle conditions [4]. These incidents
51 can lead to serious consequences, including disruptions to railway lines and the potential for loss of
52 life and property.

53 As shown in Fig. 1 (b), train derailments can cause extensive secondary damage to infrastructure
54 and the surrounding environment. For instance, when a train derails, it can damage the tracks [5],
55 vehicles [6], and other equipment along the railway line [7], potentially disrupting train services for
56 days or even weeks. In addition, a derailed train can spill hazardous materials, such as fuel, chemicals,
57 or even radioactive materials, which can pose a serious threat to nearby communities and the
58 environment [8].



59
60 Fig. 1. (a) Distribution of train derailments caused by infrastructure in [3], and (b) statistics
61 of secondary damage caused by derailed vehicles.

62 The TTS is a complex system comprising multiple sub-systems [9]. The risk of train derailment
63 depends on the quality of both railway vehicles and turnouts [10, 11]. The wheels are constrained by
64 the wheel flange, and typically derail in the form of wheel climbing or wheel jumping. To reduce the
65 likelihood of derailment during its service life, wheel load reduction rate and derailment coefficient
66 should be controlled [12]. Previous studies have individually assessed the derailment risk based on
67 examining the effect of each parameter on passive safety. For example, Ge et al. [13] developed a
68 dynamic simulation model for the TTS and revealed the effect of coupler forces and wheel-rail friction
69 coefficients on dynamic derailment risk at RTs. Burgelman et al. [14] performed a multi-body dynamic
70 simulation and examined the passive safety in a #1:9 turnout based on dynamic derailment coefficients.
71 The results showed that the lateral contact force increases significantly when braking forces are applied
72 to the front wheels, thereby increasing the risk of derailment. Lai et al. [15, 16] investigated the
73 mechanism of wheel climbing derailment and wheel jumping derailment during a vehicle passes over
74 a turnout. However, few studies have attempted to investigate the causal relationship between the
75 conditions of the TTS and the risk of derailment at RTs. Therefore, for such high derailment risk areas
76 as turnouts, there is an urgent need to quantitatively assess the derailment and develop safety
77 enhancement measures to prevent secondary damage from hazardous materials and vehicle collisions.

78 To address this gap, the objective of this study is to propose a failure probability assessment
79 method to systematically analyse derailment risk in classification yards with the uncertainty of the TTS.
80 The approach can be used to evaluate the safety of trains passing through RTs and suggest preventive

81 measures to reduce derailment risk in classification yards. The development of the proposed model
82 was based on IFFTA, and NGBN. Intuitionistic fuzzy sets (IFS) are employed to handle linguistic terms
83 obtained from different experts, which cannot be accurately expressed using probability distribution
84 functions. By utilizing the updated probabilities of input variables derived from current inspection data,
85 the Bayesian inference is capable of producing probabilities that reflect the risk of derailment at RTs.

86 The remainder of this paper is structured as follows: Section 2 provides a comprehensive review
87 of the relevant literature. Section 3 introduces the TTS and freight train derailment mechanism at RTs.
88 Section 4 presents the fundamentals of intuitionistic fuzzy Bayesian network (IFBN) and Noisy or gate
89 model. The data analysis, model verification and preventive measures are presented in Section 5.
90 Finally, conclusions, contributions, and future work are briefly summarized.

91 **2 Literature review**

92 *2.1 Fault tree analysis*

93 Various probabilistic risk assessment methods such as Fault tree analysis (FTA) [17], Event tree
94 analysis (ETA) [18], failure mode and effects analysis (FMEA) [19], Markov chains [20], Bayesian
95 network (BN) [21], and Petri nets [22] have been proposed. Among these methods, FTA is commonly
96 used for root cause analysis in multiple industries [17]. The method involves converting a physical
97 system into a structured logical graph where a sequence of basic events (BEs) leads to a specified top
98 event [17]. FTA includes both qualitative and quantitative analysis [23]. It helps assess potential failure
99 modes and causes for complex systems such as the electronics, transportation, nuclear industry, and
100 chemical industry. FTA has found valuable applications in the field of rail safety. Nguyen et al. [24]
101 employed the FTA method to assess the failure probabilities associated with potential accidents,
102 including train collisions. Huang et al. [25] introduced a combined approach that incorporated FTA and
103 fuzzy D-S evidential reasoning to investigate the risks associated with the transportation of hazardous
104 goods by rail. Jafarian et al. [26] presents a comprehensive study on the evaluation of the railway safety
105 risks using the fuzzy FTA. To assess adjacent-track accidents, Lin et al. [27] used an event tree and a
106 fault tree to identify basic events that contribute to the accidents. Esmaeeli et al. [28] used FTA and
107 event tree to evaluate the accident risk for railway transportation in Canada. Although FTA allows for
108 the identification of risk factors in railway system, they still have limitations in expressing the
109 uncertainty of event logical relations and probability updates since they are unable to capture the
110 unpredictability of risk events. Relying solely on FTA for evaluating the risk of train derailment at the
111 marshalling yard is inadequate.

112 *2.2 Intuitionistic fuzzy set theory*

113 When the necessary data, such as failure rates and probabilities, is available, the probability of the
114 undesired event can be quantified. Obtaining accurate failure probability for large and complex systems
115 is challenging because of inadequate observations and insufficient historical data. Fuzzy set theory was
116 developed by Zadeh in 1965 to deal with imprecise information and uncertainty for system safety [29].
117 This theory is an extension of the classical set that only has two states. A combination of expert
118 elicitation method and fuzzy set theory is able to be used to calculate the prior probability of BEs when
119 historical data is not available [30]. For instance, Huang et al. [25] proposed a combined approach of
120 FT and Fuzzy D-S evidential reasoning to analyse risk of railway dangerous goods transportation,
121 which addresses the issues of uncertainty modeling and information fusion during accident analysis.
122 Cheliyan et al. [31] used fuzzy FTA to analysis the failure probability of oil and gas leaks in subsea
123 production system. However, in complex decision environments, traditional fuzzy sets that only rely
124 on membership functions may result in a loss of information. In order to overcome the limitations,
125 Atanassov [32] extended conventional fuzzy sets and proposed IFS in 1986. This theory can use the
126 membership, non-membership, and degrees of hesitate to better express the uncertainty and fuzziness
127 [33]. When compared with classical fuzzy set, IFS is more effective in dealing with realistic situations
128 and modeling human thinking when compared to classical fuzzy sets [34]. The combination of the
129 expert elicitation method and IFS has been effectively utilized in various industries for risk assessment
130 [34-36].

131 2.3 Bayesian network

132 BN is one of the most efficient methods for dealing with uncertainty in complex systems. It allows
133 for easy expression of variable relationships using graphics and conditional probability tables (CPTs).
134 BN can also predict system safety with high accuracy from small data sets and update the dynamic risk
135 with new information [37]. Previous studies have shown the applicability of BN model in various fields,
136 such as chemical industry [38], ocean engineering [39], medical diagnosis [40], and civil engineering
137 [41, 42]. BN models have also been applied to fault diagnosis and failure prediction in road and railway
138 systems [43, 44]. However, there are so many risk factors for the TTS and the existing derailment
139 databases at RTs are insufficient for the BN analysis. As a result, the failure data of root nodes and
140 CPTs required for the BN parameter learning are difficult to be obtained. To overcome this shortcoming,
141 the Delphi method and Noisy-or gate model were integrated into BN approach to assist identifying
142 joint probability distribution (JPD) of a system [44, 45].

143 2.4 Risk analysis in railway classification yards

144 Cozzani et al. [46] examined three distinct types of accidents that can occur in railway yards: (i)
145 “in-transit-accident-induced” releases; (ii) “shunting-accident-induced” spills; and (iii) “non-accident-
146 induced” leaks. They developed a comprehensive risk assessment framework that combined Hazard
147 and Operability analysis with Fault Tree Analysis (FTA). Zhang et al. [47] introduced a set of three
148 control measures to enhance operational safety in classification yards. These measures encompass
149 preventive control, process control, and result control perspectives. Ye et al. [48] developed an
150 acoustic-based technology to detect the unreleased braking of freight wagons during the uncoupling
151 operation at a railway yard. Lai et al. [49] assessed the dynamic derailment risk associated with vehicle
152 retarders through numerical simulation and 3D quasi-static analysis. Chang et al. [50] observed that
153 the risk of accidents in classification yards tends to be higher due to the intricate track layout and semi-
154 automated traffic control systems. These studies have significantly contributed to enhancing safety
155 within railway yards by analyzing and evaluating various accident risks. However, it is noteworthy that
156 none of these studies have delved into the assessment of train derailments at railway turnouts (RTs)
157 within classification yards, especially considering the uncertainties associated with the TTS. Therefore,
158 there is a clear need to establish a comprehensive research framework dedicated to analyzing the risk
159 of derailments as trains pass through RTs within railway yards.

160 2.5 Application of BN and fuzzy sets in rail transportation system

161 The failure analysis for the rail transport system has been a topic of interest for researchers who
162 have tried to assess the safety of railroads from different perspectives. For instance, Liu et al. [51]
163 investigated the causal relationship between the frequency of ultrasonic rail defect inspections and the
164 risk associated with the transportation of hazardous materials on railroads. Wang et al. [52] studied the
165 risk of broken rail in freight railroads using machine learning. Ishak et al. [53] proposed a maintenance
166 strategy for turnout geometry based on risk analysis that takes into account various types of failures in
167 order to reduce the risk of derailments. Dindar et al. [44] proposed a BN-based probabilistic risk analysis
168 method for quantifying the derailment risk at RTs, particularly under extreme weather conditions. They
169 employed Buckley's confidence interval-based method to derive both marginal and conditional
170 probabilities for Bayesian Network inference. In addition, their study also provides new insights into
171 human errors, which result in derailments at RTs [54]. Inspired by their work, we have developed an
172 enhanced methodology. This approach effectively converts qualitative linguistic assessments provided
173 by experts into more reliable estimates of failure probabilities when historical data is insufficient. It is
174 designed to assess derailment risks within railway classification yards, further contributing to the
175 enhancement of railway safety.

176 **Table 1**

177 Examples of the use of BN and fuzzy sets in the area of railroad transportation safety.

Authors	Area of focus	Approaches	Key findings/marks
---------	---------------	------------	--------------------

Dindar et al. [44]	Train safety under extreme weather condition	Fuzzy set theory, BN	BN and Fuzzy Sets were employed to assess the risk of train derailment when faced with uncertain climate conditions.
Liu et al. [55]	High-speed railway accidents	IFS theory and FTA	An IFFTA model is proposed and used to quantify the risk of high-speed railway system due to the incompleteness of prior information.
Wang et al. [56]	Turnout failure prediction	Entropy Minimization, Causal noisy Max model, BN	A BN was established to forecast the weather-related failure of turnouts. The Causal Noisy Max model was utilized to handle the CPTs based on limited data sets.
Liang et al. [57]	Risk analysis on railway level crossings	BN	A new BN framework is proposed to quantify the risk associated with railway level crossings.
Castillo et al. [58]	Risk analysis of railway lines	Markovian-BN	A Markovian-BN model has been created to assess the likelihood of accidents occurring when trains pass over conventional or high-speed railway lines, considering the possibility of human error.
Huang et al. [59]	Hazardous goods transportation	BN, Interpretive Structural Modeling (ISM)	An approach based on ISM and BN was utilized to analyse the degree of interaction between various risk factors involved in the transportation of hazardous goods by railway.
Panrawee et al. [60]	Railway accidents	BN, decision tree, petri-net	A Bayesian approach has been adopted to cope with uncertainties of railway accident and the model is validated using petri-net and decision tree

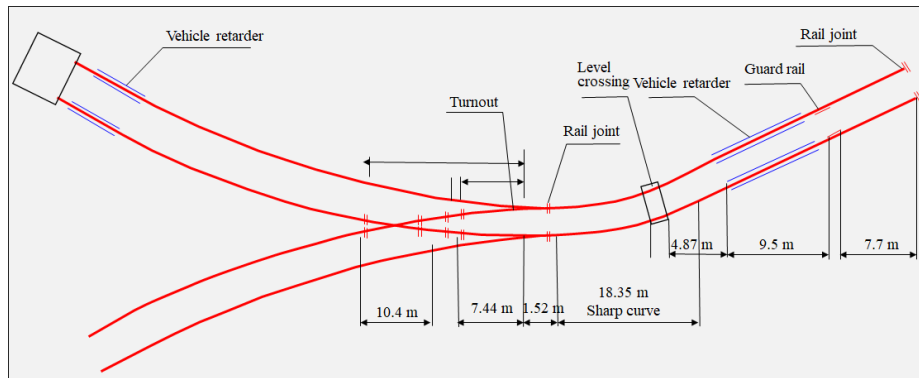
178 **Table 1** presents some typical examples of research results related to the application of BN and
179 fuzzy sets in the field of railroad transportation safety. These studies have shown that BN model has
180 good capability for the risk quantification in the field of railway transportation, such as track failure
181 estimation, dangerous goods transportation and collision accident analysis. There are also some gaps
182 need to be filled. In the process of expert judgement, uncertainties and hesitations can arise when
183 determining the membership of classical fuzzy sets. Using IFS can better express the fuzziness and
184 uncertainty from expert opinions. Furthermore, for a complex BN structure with too many nodes and
185 directed arcs in this study, there may be inadequate accident data in railway yards for the CPT
186 estimation. To address this limitation, we integrated BN with the Noisy-or gate model to reveal the
187 causal relationship and derailment risk when railway vehicles run in railway yards under uncertainties.

188 3 Material and background

189 3.1 Brief introduction of TTS

190 The TTS is composed of several crucial sub-systems that work in conjunction to guarantee the
191 secure operation of trains. The TTS comprises of three main sub-systems: the train sub-system, the
192 turnout sub-system, and the wheel-rail contact module. The train sub-system primarily consists of
193 multiple wagons, bogies, wheelsets, and couplers. The turnout sub-system, on the other hand, guides
194 and supports vehicles. It is a complex system comprised of a variety of track components, including
195 rails, fasteners, ballast, switches, crossings, and other related components. This paper has taken into
196 account the switch section, closure section, and frog section in risk analysis. In addition, as the turnout
197 is a combination of multiple rails, the wheel-rail relationship at RTs is complex and random. The
198 vehicle retarders are installed in front of turnouts at classification yards in China as a measure to reduce
199 train speed, as illustrated in Fig. 2. The presence of sharp curves and vehicle retarders before the turnout

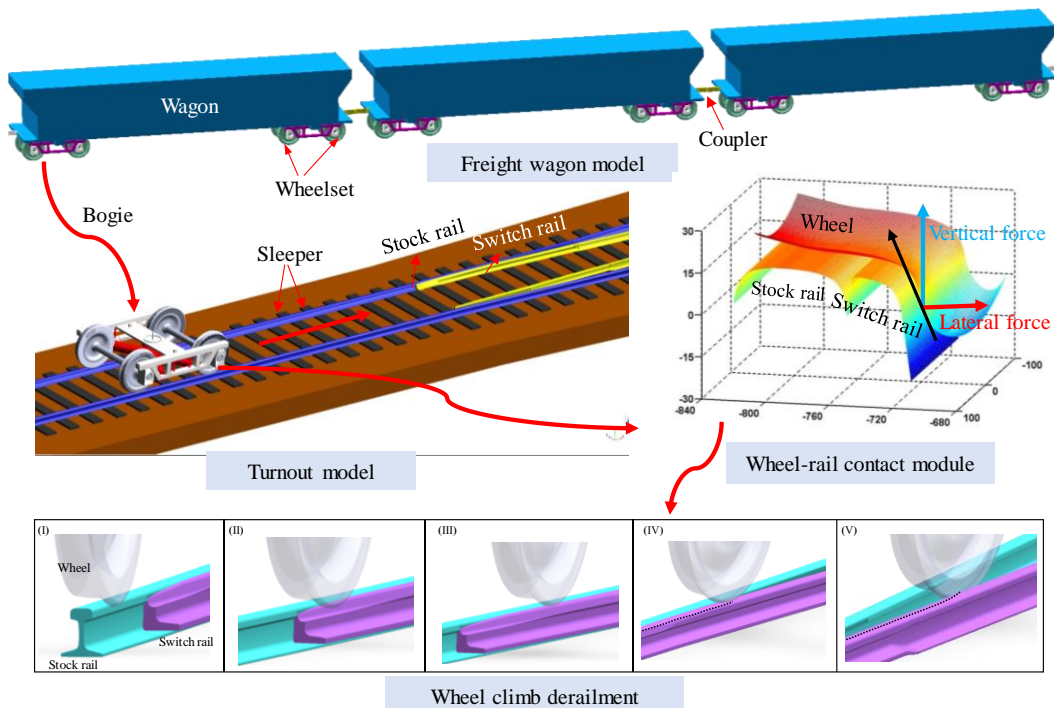
200 can also decrease train running safety. The contact between the wheels and rails can significantly
 201 impact the safety [61]. For instance, when contact points shift to the wheel flange, wheels may climb
 202 up to railhead and cause a derailment [11]. Furthermore, intense impacts between the wheels and
 203 turnouts are very common due to the discontinuities of the track, which can result in the wheel jumping
 204 to the railhead.



205
 206 Fig. 2. Schematic diagram of the track alignment at classification yard in China.

207 *3.2 Derailment mechanism at RTs*

208 When a wheel passes over a RT, it needs to pass over a split rail in order to follow the correct
 209 track. However, if the relationship of the wheel-rail contact is abnormal, it can cause the wheel to derail.
 210 Fig. 3 illustrates a diagram of derailment processes when railway vehicles pass through the railway
 211 switch. The process of a wheel derailing on a switch typically involves the wheel climbing up the
 212 switch rail instead of following the intended path. This can cause the wheel to lose contact with the rail
 213 and potentially cause damage to the switch and surrounding tracks. As the wheel continues to move
 214 forward, it can then fall off the rail completely or get stuck in a position where it cannot move any
 215 further. This can cause a delay in train traffic as crews work to remove the derailed wheel and repair
 216 any damage caused. It is noted that when vehicles are traveling at high speeds, it may cause the carriage
 217 to overturn, leading to the spread of hazardous materials. Overall, derailments at turnouts can be caused
 218 by different factors, such as mechanical issues with the rail switch, poor maintenance of the track, or
 219 vehicle component failure. The occurrence of any abnormal states between them may cause the railway
 220 vehicle to derail at turnouts.

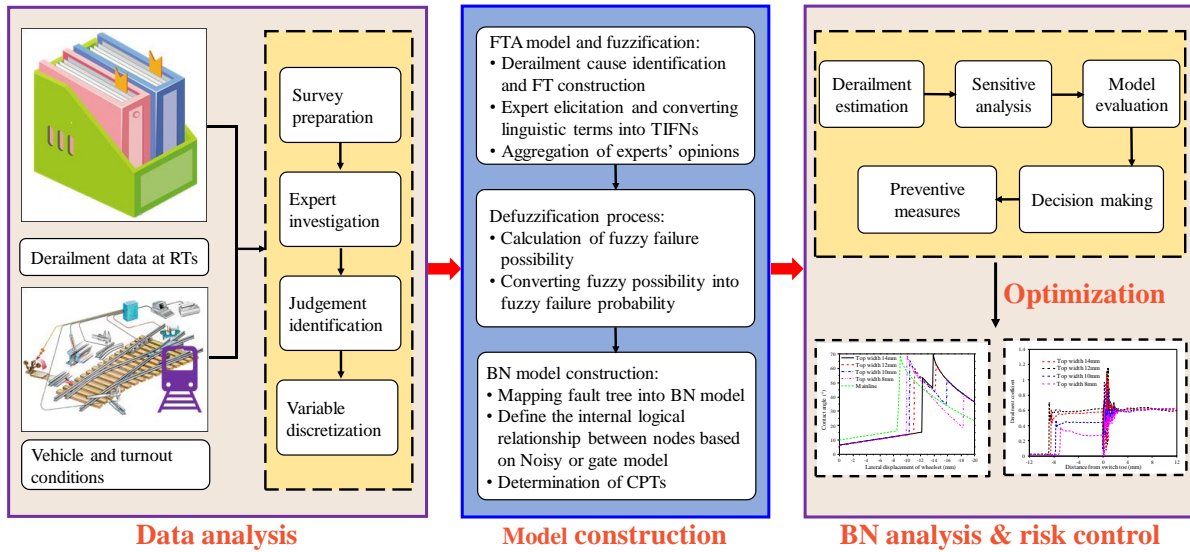


221

222 Fig. 3. A simplified diagram of wheel derailment processes at RTs.

223 **4 Proposed IFFTA and NGBN methodology**

224 The approach for derailment risk analysis is based on the IFFTA model, the Noisy or gate, and the
 225 BN model. Fig. 4 illustrates the research framework for the proposed methodology. Firstly, a fault tree
 226 is constructed. Secondly, opinions from different experts are collected and corresponding linguistic
 227 terms for BEs are quantified as TIFNs. An improved aggregation method is then introduced to
 228 aggregate the TIFNs, which has considered the effect of experts' weight degree of consensus. Thirdly,
 229 the fuzzy failure probability of BEs can be calculated and the fault tree is mapped into the BN structure.
 230 The Noisy-or gate modeling is then introduced and integrated into the naïve BN model to derive the
 231 CPTs. Finally, Bayesian inference, sensitivity analysis, model verification, and preventive measures
 232 are presented. The details are presented as follows.

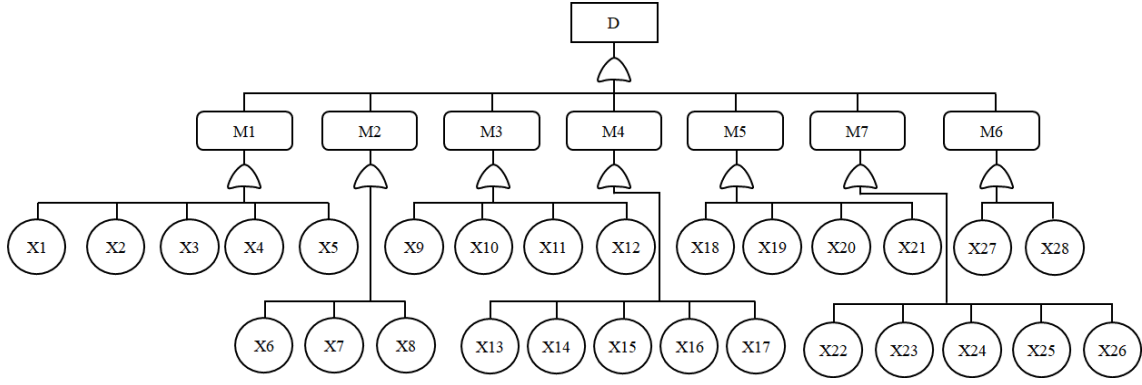


233 **Data analysis** **Model construction** **BN analysis & risk control**
 234 Fig. 4. Flowchart of proposed methodology.

235 **4.1 Derailment cause identification and FT construction**

236 Identifying risk factors for TTS is a critical step in analysing the risk of the train derailment at
 237 RTs. It represents the first step in conducting a reliability analysis. Typically, hazards and operability
 238 analysis [62] and FMEA [63] are two common methodologies used for identifying potential hazards in
 239 industrial processes and systems. In this paper, the risk factors are determined by analysing historical
 240 data from 27 derailment cases that occurred at RTs from 2014 and 2019. Besides, literature [3, 4, 64],
 241 and expert judgment are also utilized to identify the risk factors.

242 A fault tree for the train derailment at RTs is shown in Fig. 5. The diagram is divided into three
 243 levels: (1) BEs are at the lowest level, (2) intermediate events (IEs) are at the middle level, and (3) top-
 244 level event (TE) is at the top level. The connections between various events are represented by logical
 245 symbols. In this study, the derailment risk at RTs is designated as the top event for the risk analysis of
 246 derailment. The full name of each abbreviation in the fault tree is provided in Section 5.2.



247

248 Fig. 5. The fault tree for the train derailment at RTs.

249 4.2 Introduce IFS to obtain probability of BEs

250 For the quantification analysis of derailment risk at RTs, the accurate prior probability of root
 251 nodes should be obtained. The probability of an event occurring can be determined using various
 252 methods such as statistical analysis, historical data, and expert elicitation. Note that accurate historical
 253 data for the TTS in this study is insufficient. Thus, the combined approach of expert elicitation and IFS
 254 is a good choice for identifying the failure probability of the BEs. The detailed procedures for
 255 determining the fuzzy failure probability of BEs are presented as follows.

256 4.2.1 Concept of IFS theory

257 **Definition 1:** Intuitionistic fuzzy set.

258 If X is a universe of discourse, the IFS \tilde{A} in X can be expressed as [32]:

259
$$\tilde{A} = \left\{ \langle x, u_{\tilde{A}}(x), v_{\tilde{A}}(x) \rangle \mid x \in X \right\} \quad (1)$$

260 where: $u_{\tilde{A}}(x): X \rightarrow [0,1]$ and $v_{\tilde{A}}(x): X \rightarrow [0,1]$ represent the membership function and non-membership
 261 function of \tilde{A} . The functions satisfy the following two conditions:

262
$$u_{\tilde{A}}(x) + v_{\tilde{A}}(x) \in [0,1], \quad \forall x \in X \quad (2)$$

263
$$\pi_{\tilde{A}}(x) = 1 - u_{\tilde{A}}(x) - v_{\tilde{A}}(x) \quad (3)$$

264 where $\pi_{\tilde{A}}(x)$ represents the IF index of $x \in \tilde{A}$, also referred to as the degree of uncertainty or level of
 265 hesitation.

266 **Definition 2:** Intuitionistic fuzzy number.

267 Convex intuitionistic fuzzy set [32]:

268 Membership functions of $u_{\tilde{A}}(x)$ of \tilde{A} is fuzzy-convex i.e.

269
$$u_{\tilde{A}}(\lambda x_1 + (1 - \lambda)x_2) \geq \min \{u_{\tilde{A}}(x_1), u_{\tilde{A}}(x_2)\} \quad \forall x_1, x_2 \in X, \quad 0 \leq \lambda \leq 1 \quad (4)$$

270 Non-membership functions of $v_{\tilde{A}}(x)$ of \tilde{A} is fuzzy-concave i.e.

271
$$v_{\tilde{A}}(\lambda x_1 + (1 - \lambda)x_2) \leq \max \{v_{\tilde{A}}(x_1), v_{\tilde{A}}(x_2)\} \quad \forall x_1, x_2 \in X, \quad 0 \leq \lambda \leq 1 \quad (5)$$

272 A triangular-shaped intuitionistic fuzzy number (TIFN) can be denoted as Eqs. (6) and (7). The
 273 shape of TIFN is shown in Fig. 6.

$$274 \quad u_{\tilde{A}}(x) = \begin{cases} \frac{x-a}{b-a}, & a \leq x \leq b \\ \frac{c-x}{c-b}, & b \leq x \leq c \\ 0, & \text{otherwise} \end{cases} \quad (6)$$

$$275 \quad v_{\tilde{A}}(x) = \begin{cases} \frac{b-x}{b-a'}, & a' \leq x \leq b \\ \frac{x-b}{c'-b}, & b \leq x \leq c' \\ 1, & \text{otherwise} \end{cases} \quad (7)$$

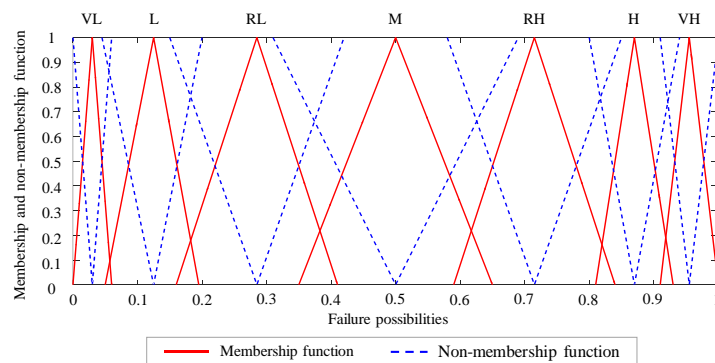
276 where the TIFN is expressed by $\tilde{A} = (a, b, c; a', b, c')$.

277 4.2.2 Expert elicitation and IF-fuzzification

278 Expert elicitation can be used as an alternative statistical method when data is not available or
 279 unreliable, and it relies on expert knowledge and judgment to estimate probabilities. It is also one of
 280 the efficient methods for supporting system reliability analysis. In this study, the knowledge from
 281 multi-experts is utilized to obtain fuzzy failure probabilities (FFP) of BEs. The expert judgment method
 282 describes the probability of BEs by dividing the probability range into k regions and matching the
 283 corresponding linguistic terms. In this work, it is divided into 7 levels of linguistic terms, which consist
 284 of very low (VL), low (L), reasonably low (RL), moderate (M), reasonably high (RH), high (H), and
 285 very high (VH). Besides, based on the historical derailment data in classification yards, we have
 286 categorized the derailment risk into seven levels based on the frequency of train derailments.
 287 The probability range is from $6.61e-6$ to $1.10e-1$, as shown in **Table 2**. The annual frequency is
 288 determined by the fuzzy possibility score and fuzzy failure probability in Eqs. (16-18). Fig. 6
 289 illustrates the graphical representation of all the potential failure scenarios.

290 **Table 2**
 291 Risk level for derailment at RTs in classification yards.

Risk level	Description	Annual frequency
Very high	≥ 1 derailment accident per month during operations	$>1.10e-01$
High	≥ 1 derailment accident per quarter of a year during operations	$2.60e-02 \sim 1.10e-01$
Reasonably high	≥ 1 derailment accident per half-year during operations	$5.20e-03 \sim 2.60e-02$
Moderate	≥ 1 derailment accident per year during operations	$1.00e-03 \sim 5.20e-03$
Reasonably low	≥ 1 derailment accident in 2 years during operations	$1.92e-04 \sim 1.00e-03$
Low	≥ 1 derailment accident in 5 years during operations	$4.71e-05 \sim 1.92e-04$
Very low	≥ 1 derailment accident in 10 years during operations	$6.61e-06 \sim 4.71e-05$



292

294 4.2.3 Aggregation of expert opinions

295 Given that the selected experts possess diverse backgrounds, experiences, and levels of expertise,
 296 their judgments on the risk level of BEs may be different. In order to obtain a unique intuitionistic
 297 fuzzy failure possibility, their opinions should be aggregated. In this study, we utilize the Similarity
 298 Aggregation method (SAM) [65] to aggregate the linguistic terms of a group of experts. **Table 3** is
 299 used to determine the weighting scores (WS) of experts in this study. It should be noted that the term
 300 "worker" refers to a young employee who has just joined the railroad company and lacks sufficient
 301 work experience. The details for the aggregation method are presented as follows:

302 Step 1. The similar degree of opinions \tilde{A}_i and \tilde{A}_j from experts E_i and E_j can be expressed as $S(\tilde{A}_i, \tilde{A}_j)$,
 303 and it can be calculated by Eq. (8):

$$304 \quad S(\tilde{A}_i, \tilde{A}_j) = \begin{cases} KW(A_i) / KW(A_j), & \text{if } KW(A_i) \leq KW(A_j) \\ KW(A_j) / KW(A_i), & \text{if } KW(A_i) \geq KW(A_j) \end{cases} \quad (8)$$

$$305 \quad KW(\tilde{A}_i) = \frac{(a_i + a'_i) + 4b_i + (c_i + c'_i)}{8} \quad (9)$$

306 where $KW(A_i)$ and $KW(A_j)$ denote the expectancy evaluation for TIFNs \tilde{A}_i and \tilde{A}_j respectively.

307 The similarity matrix (SM) can be obtained in the following form when there are m experts:

$$308 \quad SM = \begin{bmatrix} 1 & S_{12} & S_{13} & \cdots & S_{1m} \\ S_{21} & 1 & S_{23} & \cdots & S_{2m} \\ \vdots & \vdots & \vdots & \cdots & \vdots \\ S_{m1} & S_{m2} & S_{m3} & \cdots & 1 \end{bmatrix} \quad (10)$$

309 A larger value of S_{ij} represents a higher degree of consistency between the opinions of the experts.
 310 Conversely, if $S_{ij} = 0$, it means that there is no overlap or intersection between the opinions of the
 311 experts.

312 Step 2. The average agreement degree of each expert E_i is obtained as

$$313 \quad AA(E_i) = \frac{1}{m-1} \sum_{\substack{j=1 \\ j \neq i}}^m S_{ij}, \quad i = 1, 2, \dots, m \quad (11)$$

314 Step 3. The relative agreement degree (RAD) for each expert E_i can be calculated as

$$315 \quad RAD(E_i) = \frac{AA(E_i)}{\sum_{i=1}^m AA(E_i)}, \quad i = 1, 2, \dots, m \quad (12)$$

316 Step 4. Weighting factor (WF)

317 The WF for each expert is calculated based on four criteria, including professional position, years
 318 of work experience, educational level, and age. This approach improves the credibility of the data by
 319 assigning different weights to each expert, instead of treating all experts as equal. Thus, five experts
 320 are selected from the field of railway engineering, who come from universities, maintenance
 321 departments, safety management, each expert has a distinct WS. Firstly, entropy technology is utilized
 322 to determine the importance weights of the four criteria [66]. And then, the WF of expert E_i is calculated
 323 based on Eq. (13).

$$324 \quad WF(E_i) = \frac{WS(E_i)}{\sum_{i=1}^m WS(E_i)}, \quad i = 1, 2, \dots, m \quad (13)$$

325 Step 5. Aggregated weight calculation.

326 The weight of the aggregated opinions is calculated by combining the $WF(E_i)$ and $RAD(E_i)$ of
 327 each expert E_i , as shown in Eq. (14).

$$328 \quad CC(E_i) = \beta \cdot WF(E_i) + (1 - \beta) \cdot RAD(E_i) \quad (14)$$

329 where β ($0 \leq \beta \leq 1$) denotes the relaxation factor, which represents the importance expert weight and
 330 relative degree of agreement.

331 Step 6. Aggregated results.

332 The intuitionistic fuzzy aggregation results of expert opinions can be calculated by Eq. (15) [67].

$$333 \quad \tilde{R}_{AG} = \sum_{i=1}^m (\oplus T_{\omega}) CC(E_i) \cdot \tilde{A}_i \quad (15)$$

334 **Table 3**

335 Weighting score for experts.

Attributes					Score
Professional position	Service time	Education level	Age		
Senior academic, Chief Engineer, Director	>20 years	PhD	>60		5
Junior academic, Manager Engineer	15-20 10-14	Master Bachelor	50-60 40-49		4 3
Technician	5-9	HND	30-39		2
Worker	<5	School-level	<30		1

336 4.2.4 IF-defuzzification

337 The aggregated TIFN $\tilde{A} = (a, b, c; a', b, c')$ of the BE can be defuzzified by the center of area method
 338 [68]. The processes of transforming TIFN into FFP through defuzzification are divided into two stages:
 339 converting the TIFN into a fuzzy possibility score (FPS), and then converting the FPS into FFP. It can
 340 be expressed as follows:

$$341 \quad FPS = \frac{1}{3} \left[\frac{(c' - a')(b - 2c' - 2a') + (c - a)(a + b + c) + 3(c'^2 - a'^2)}{c' - a' + c - a} \right] \quad (16)$$

342 4.2.5 Converting FPS into FFP

343 In order to obtain the FFP, the IF-defuzzification procedure generates an FPS that signifies the
 344 likelihood of BEs taking place. Onisawa [69] proposed a conversion method, whereas it is not
 345 universally applicable across different industries. This work utilized an improved approach to compute
 346 the FFP using Eqs. (17) and (18), taking into account that the failure likelihood is segmented into seven
 347 distinct regions.

$$348 \quad FFP = \begin{cases} 1/10^K & FPS \neq 0 \\ 0 & FPS = 0 \end{cases} \quad (17)$$

$$349 \quad K = \begin{cases} -0.721 \ln FPS + 2.839, & 0 \leq FPS < 0.2 \\ -1/3 \times (10FPS - 14), & 0.2 \leq FPS \leq 0.8 \\ [(1 - FPS) / FPS]^{0.445} \times 3.705, & 0.8 < FPS \leq 1 \end{cases} \quad (18)$$

350 The derivation of the coefficient K can be found in Ref. [67]. This method was originally
 351 proposed and validated to deal with the probability of failure of human-machine systems.
 352 Inspired by the method [67], the modified coefficient is determined based on the seven-level
 353 probability regions provided in Table 2. The proposed method could avoid the subjective
 354 understanding deviation that arises when converting qualitative empirical knowledge from

355 domain experts into quantitative failure probability.

356 4.3 Bayesian modeling

357 4.3.1 Bayesian network

358 BN is a type of graphical model that utilizes a directed acyclic graph to depict a series of variables
359 and their conditional dependencies. Each node in the graph represents a variable and the edges between
360 the nodes represent the probabilistic relationships between the variables. BN can be used to represent
361 causal relationships, represent uncertainty and perform probabilistic inference. It can be used to
362 calculate the probability of a variable given the evidence provided by observed variables and the known
363 relationships encoded in the network structure [70]. Besides, one can perform probabilistic inference
364 to calculate the failure probability for the overall system. Additionally, sensitivity analysis can be
365 conducted to understand how changes in component failure probabilities impact the system reliability.
366 Overall, a BN model that combines IFFTA is a flexible approach for derailment risk analysis because
367 it can handle complex systems with multiple interacting components and uncertainties in the failure
368 probabilities. The JPD of a group of nodes can be defined as Eq. (19), taking into account the
369 conditional dependencies and chain rules [70].

$$370 P(X) = P(X_1, X_2, \dots, X_n) = \prod_{i=1}^n P(X_i | \text{Parent}(X_i)) \quad (19)$$

371 The conditional probability can be expressed as follows:

$$372 P(A|B_i) = \frac{P(AB_i)}{P(B_i)} \quad (20)$$

373 The BN updates the occurrence probability (prior) of root nodes based on new evidence using
374 Bayes' theorem. The updated probability (posterior) of the root nodes is expressed as:

$$375 \pi(B_i) = \frac{P(AB_i)}{P(A)} = \frac{P(B_i)P(A|B_i)}{\sum_{i=1}^n P(B_i)P(A|B_i)} \quad (21)$$

376 After obtaining the prior probability and posterior probability, the critical root nodes can be
377 determined by ratio of variation (RoV), as shown in Eq. (22).

$$378 RoV(X_i) = \frac{\pi(X_i) - \theta(X_i)}{\theta(X_i)} \quad (22)$$

379 Where $\pi(X_i)$ represents posterior probability, and $\theta(X_i)$ is prior probability.

380 4.3.2 Mapping fuzzy fault tree model into BNs

381 The process of mapping FT into BN involves two stages, which are graphical mapping and
382 numerical mapping, as shown in Fig. 7. The root nodes in BN are equivalent to the bottom events in
383 FT, while the leaf node in BN is equivalent to the top event in FT. In numerical mapping, the fuzzy
384 failure probability of each bottom event in FT is assigned as the prior probability of the corresponding
385 root node in BN. The CPT is made for the intermediate nodes and leaf node, and it is determined
386 according to the type of gate.

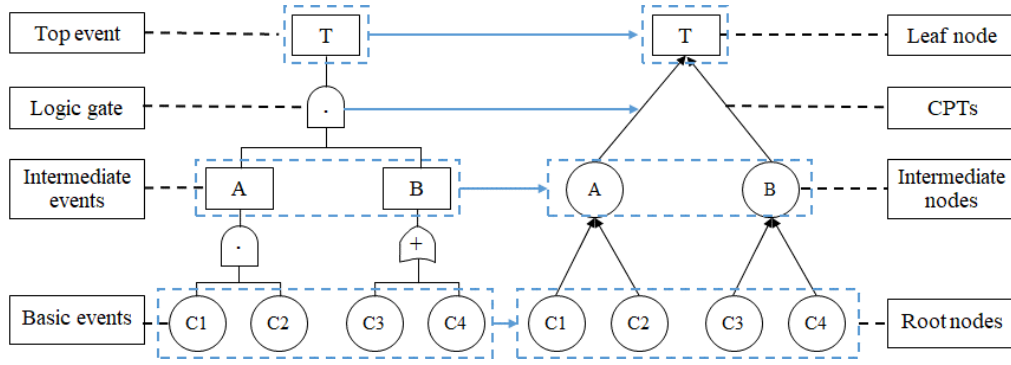


Fig. 7. Mapping process from FT into BN.

4.3.3 Noisy-or gate model

In the FTA model, logical 'OR' and 'AND' gates are used to derive the probability of occurrence. However, logic gate analysis describes the relationship between BE and IE in a very absolute way (0 or 1), in practice, it is not a simple binary. Besides, when assessing the risk of train derailment at RTs, many classification yards have not yet established a complete risk database. The use of the Noisy-or gate model allows for the derivation of CPTs with small data sets, enabling a more accurate assessment of system risk [71]. It is an interaction model used to describe the relationship between n parent nodes B_1, B_2, \dots, B_n and child node T . The model must satisfy the two assumptions when applying Noisy-or gate model for BN inference. Then the conditional probability of node T can be calculated using Eq. (23).

$$P(T = Y|B_i) = 1 - \prod_{i: X_i \in X_T} (1 - P_i) \quad (23)$$

In the actual analysis, besides the set B , there are other unknown factors that cannot be effectively identified in the risk factors that affect node T . It needs to use the extended Leaky Noisy-or gate model to attribute all risk factors that cannot be effectively identified to one factor B_L , and its connection probability is the Leaky probability, which is denoted as P_L .

The CPT of node T can be further expressed as Eq. (24).

$$P(T = Y|B_i) = 1 - (1 - P_L) \prod_{i: X_i \in X_T} (1 - P_i) \quad (24)$$

The Leaky Noisy-or gate model can also be used to determine the connection probability of the parent nodes. Assume that the network consists of two parent nodes, which could be expressed as variables C_i and C_{all} . The probabilities of occurrence of them are P_i and P_{all} , respectively. Eq. (25) can be obtained based on Eq. (23). Then, substitute Eq. (26) into Eq. (25), the connection probability is calculated by Eq. (27).

$$P(Y|C_i) = 1 - (1 - P_i)(1 - P_{all}) = P_i + P_{all} - P_i P_{all} \quad (25)$$

$$P(Y|\overline{C_i}) = P_{all} \quad (26)$$

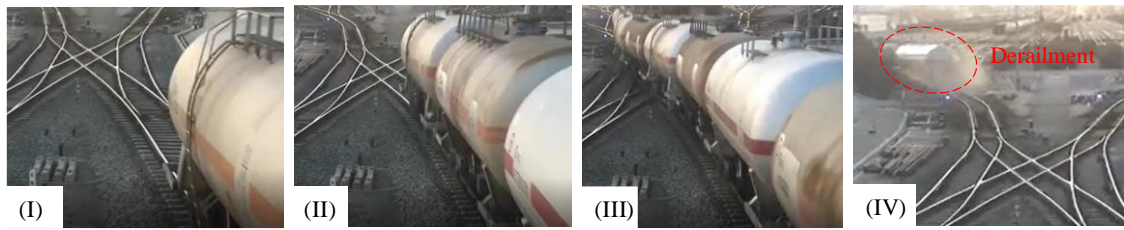
$$P_i = \frac{P(Y|C_i) - P(Y|\overline{C_i})}{1 - P(Y|\overline{C_i})} \quad (27)$$

5 Engineering application: A case study in China

5.1 Derailment scenario description

The appendix A provides examples of ten derailment incidents that occurred at low-speed RTs

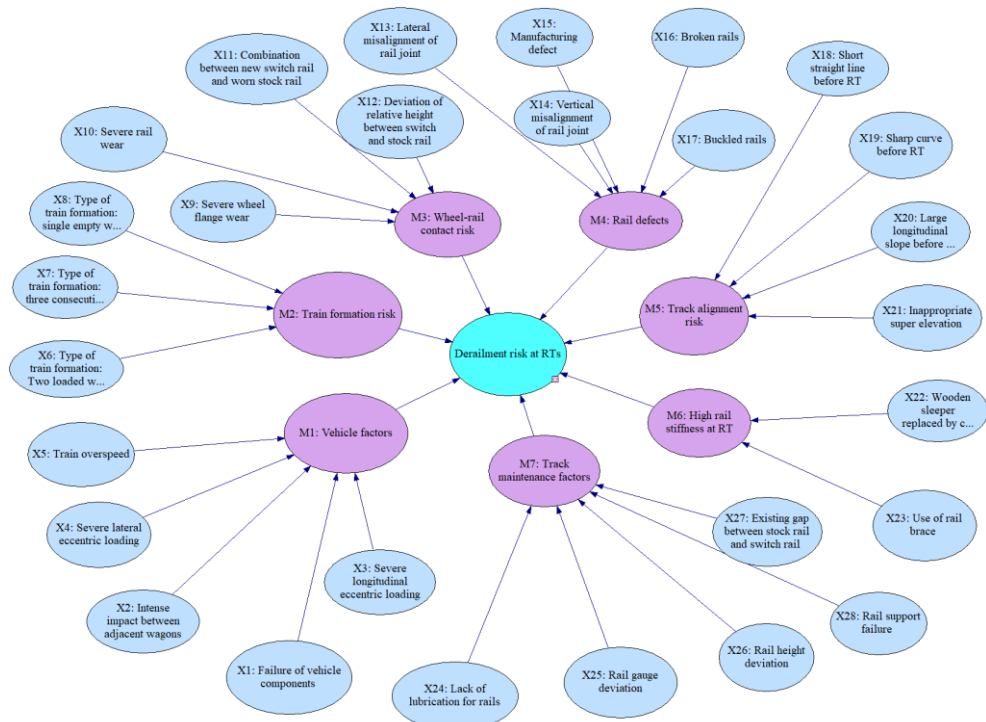
417 from March 2014 to March 2019. Fig. 8 shows a freight wagon carrying hazardous materials derailed
 418 in the turnout area at Taiyuan North marshalling station. A derailment scenario depicted in Fig. 8 (IV)
 419 shows that when the rear freight wagon passes through the turnout, the leading wheelset of the wagon
 420 begins to climb the rail at the front of the switch rail and then drops down on the sleepers at the heel
 421 of the switch rail. Based on the field investigation, the leading wheel eventually fell off the top of the
 422 rail 6.2 m from the toe of the rail switch and the wagon stopped after traveling 12 m on the sleepers,
 423 as shown in Fig. 8 (IV). The turnout is located at the front of a sharp curve with a radius of 180 m.
 424 When inspecting the condition of the track, it was found that the workers did not maintain the geometry
 425 of the turnout in time. Besides, the combination of the new switch rail and the worn stock rail results
 426 in poor wheel-rail relationships between the wheel and the rail, which increases the risk of derailment.
 427 These indicate that the poor conditions of both the vehicles and the tracks can increase the risk of
 428 derailment. Based on this analysis, it is recommended to consider factors such as vehicle abnormal
 429 responses, track alignments, train formation types, turnout defects, inappropriate wheel-rail contact
 430 interface, and track maintenance in risk assessment of derailment.



431
 432 Fig. 8. A freight wagon carrying hazardous materials derailed in the turnout area.

433 5.2 Construction of BN model

434 The potential factors that contribute to derailment risk at RTs have been analysed through expert
 435 judgment, literature review and accident reports. The identified risk factors were grouped into seven
 436 categories, including poor vehicle conditions (M1), train formation risk (M2), abnormal wheel-rail
 437 contact (M3), turnout defects (M4), track alignment risk (M5), high rail stiffness at RT (M6), and lack
 438 of track maintenance (M7). To evaluate the derailment probability, a BN model was developed, with
 439 28 root nodes, 7 intermediate nodes, and one target node. The complete BN model was constructed
 440 adopting GeNIe software, and is presented in Fig. 9. The details of each root node are listed in
 441 Appendix B.



442

444 5.3 Parameters determination

445 Before beginning Bayesian analysis, it is necessary to determine the accurate prior probability of
 446 root nodes. Expert judgments for the BEs are provided in Appendix B. Based on the calculation
 447 procedure in section 4.2.3, the aggregation results from multi-experts and corresponding FFP of the
 448 BEs are presented in Appendix B. In addition, an example of calculation results for CPT of node M5
 449 can be derived using Noisy or gate model, as shown in **Table 5**. If we define $P(M5|X18) = 0.92$,
 450 $P(M5|\bar{X}18) = 0.82$, $P(M5|X19) = 0.96$, $P(M5|\bar{X}19) = 0.70$, $P(M5|X20) = 0.95$, $P(M5|\bar{X}20) = 0.83$,
 451 $P(M5|X21) = 0.63$, $P(M5|\bar{X}21) = 0.30$. The connection probability between parent node M5 and child
 452 nodes X18, X19, X20, and X21 can be calculated by Eq. (27). The variable x_i , which is not known,
 453 follows a Gaussian probability distribution with a confidence level of 99%.

454 **Table 4**

455 Connection probability of M5.

Node	State			
X18	Y	N	N	N
X19	N	Y	N	N
X20	N	N	Y	N
X21	N	N	N	Y
$P(M5=Y X_i)$	0.56	0.87	0.71	0.47

456 **Table 5**

457 The CPT of Node M5.

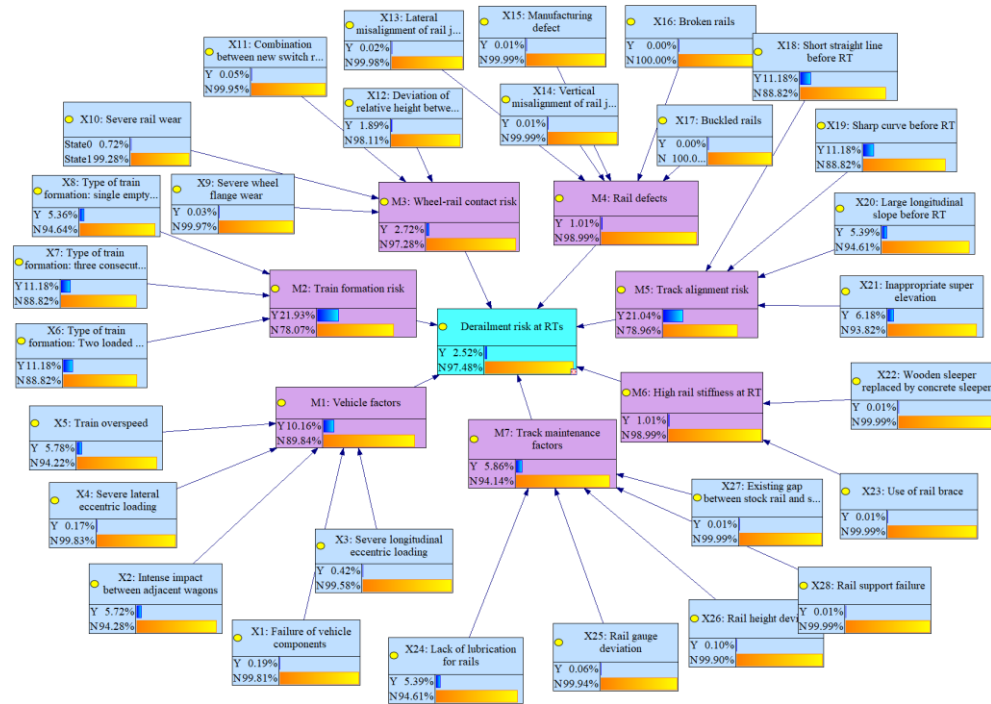
X18	X19	X20	X21	$P(M5=Y X_i)$	$P(M5=N X_i)$
Y	Y	Y	Y	0.99	0.01
Y	Y	Y	N	0.98	0.02
Y	Y	N	Y	0.97	0.03
Y	Y	N	N	0.94	0.06
Y	N	Y	Y	0.93	0.07
Y	N	Y	N	0.87	0.13
Y	N	N	Y	0.77	0.23
Y	N	N	N	0.56	0.44
N	Y	Y	Y	0.98	0.02
N	Y	Y	N	0.96	0.04
N	Y	N	Y	0.93	0.07
N	Y	N	N	0.87	0.13
N	N	Y	Y	0.85	0.15
N	N	Y	N	0.71	0.29
N	N	N	Y	0.48	0.52
N	N	N	N	0.01	0.99

458 5.4 Bayesian network inference

459 Once the IFBN structure and parameters were determined, the prediction of derailment risk at RTs
 460 was carried out using an academic version of GeNIe. The derailment probability is estimated to be
 461 2.52%, as shown in Fig. 10. In other words, this indicates that the risk level at Taiyuan North yard is
 462 high risk. To obtain the posterior probabilities of the root nodes and identify key events, probability
 463 updates are performed by introducing evidence into the BN. When the occurrence probability of
 464 'derailment risk at RTs' is set to 100%, the updated probabilities of root nodes could be calculated. Fig.
 465 11 illustrates the comparison between the prior and posterior probability of the root nodes. It is

466
467

observed the posterior probabilities of some root nodes increase significantly, which represent the critical role in causing derailment risk.



468

Fig. 10. The prediction result of derailment probability at RTs based on IFBN.

469

470

The RoV can be further calculated based on Eq. (22). As shown in Fig. 12, the critical basic events include node X2 (intense impact between adjacent wagons), node X10 (severe rail wear), node X11 (twist of track), node X5 (train overspeed), node X1 (failure of vehicle components), node X12 (deviation of relative height between switch and stock rail), and node X4 (lateral deviation of vehicle center of gravity). Thus, all of these factors need to be given more attention when trains pass through RTs.

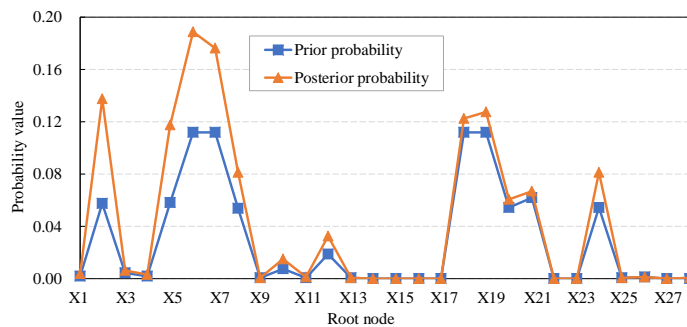
471

472

473

474

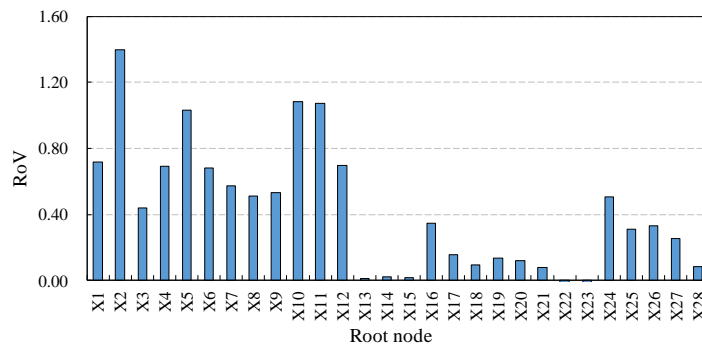
475



476

477

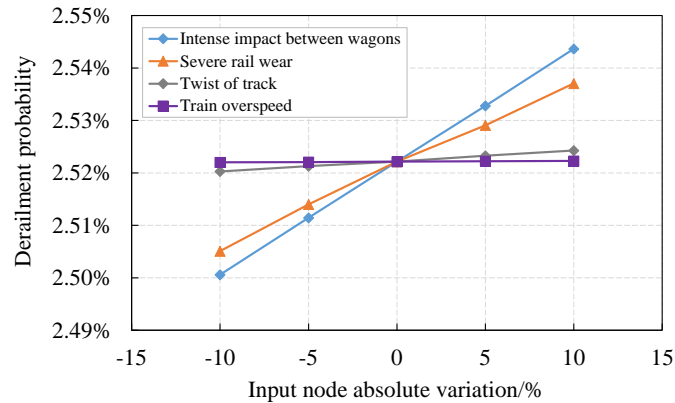
Fig. 11. Comparison of prior probability and posterior probability of root nodes.



478

480 5.5 Sensitive analysis

481 Sensitivity analysis measures the sensitivity, or responsiveness, of model results to changes in
 482 inputs. The nodes that have a significant effect on the derailment risk at RTs are shown in Fig. 12. By
 483 changing the probability of the nodes of X2, X10, X11, and X5, we obtained the sensitivity value of
 484 each node. Fig. 13 depicts the sensitivity of various variables to derailment risk at RTs. As seen in Fig.
 485 13, a slight increase or decrease in the prior probability of the parent nodes, and intense longitudinal
 486 impact load between adjacent wagons, leads to a relative increase or decrease in the child node
 487 (derailment probability at RTs). Thus, the longitudinal impacts caused by the vehicle retarder should
 488 be controlled.



489

490

Fig. 13. Sensitivity for derailment probability at RTs against other variables.

491 To obtain the influence of the risk factors on derailment risk at RTs, we further utilized the GeNIe
 492 software to conduct a sensitivity analysis of the TTS by using backward reasoning for the IFBN model.
 493 Fig. 14 shows the tornado graph in GeNIe and the target node is set to 'derailment risk at RTs'. The
 494 length of the bar indicates the extent of variation in the target state when the probabilities of all other
 495 nodes change by 100%. In addition, the green bar expresses the positive influence and the red bar
 496 reflects the negative impact. The longer the bar, the greater the influence of the cause on the result. The
 497 20 most influential factors are presented. As illustrated in Fig. 14, it is observed that the state of
 498 'Derailment risk at RTs' being Y can be changed from 0.0185 to 0.517. We can notice that
 499 $P(\text{Derailment}=Y|M1=N, M2=N, M3=N, M4=N, M5=N, M6=N, M7=N)$ impacts $P(\text{Derailment}=Y)$
 500 most. Namely, $P(\text{Derailment}=Y)$ decreases from 0.517 to 0.0185 as M1 to M7 are checked as N. The
 501 results indicate that node M1, node X2, node M3, node X5, node X10, node X11, and node X6 have a
 502 great influence on the derailment risk at RTs. This is in agreement with historical statistics in Taiyuan
 503 North marshalling station.

504

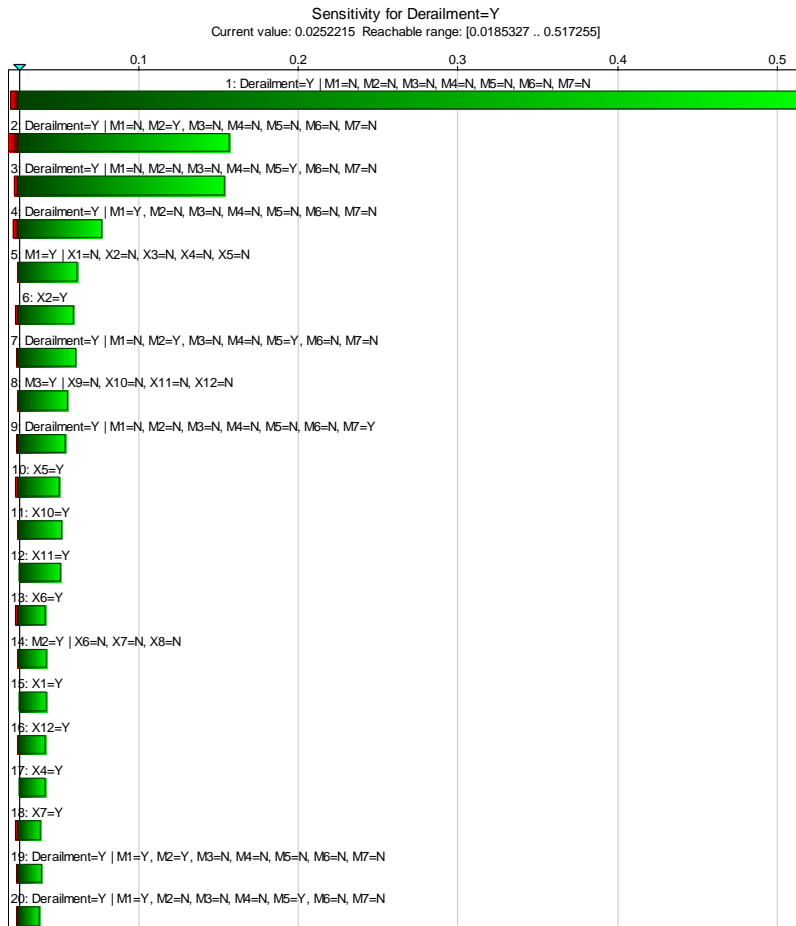
505

506

507

508

Railroad managers have responded to these critical events by taking targeted measures. These
 measures involve timely development of in-service inspections, preventive testing, and maintenance
 of vehicles and turnouts, as well as timely replacement of defective and degraded turnout components.
 Moreover, they have optimized the track parameters in the vicinity of turnouts to reduce the risk of
 derailment.

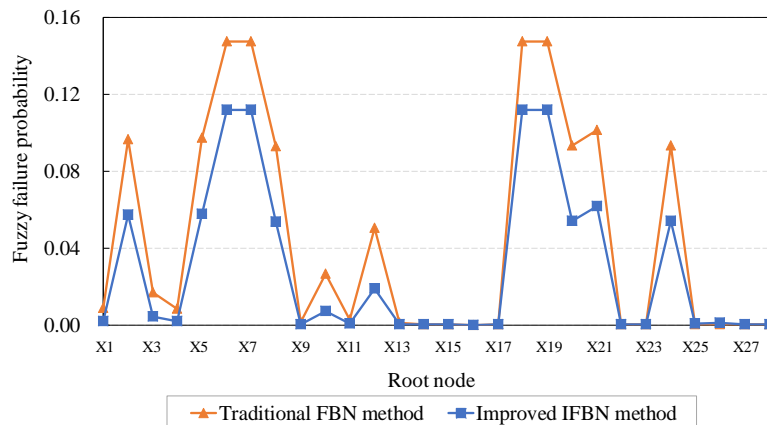


509
510

Fig. 14. Tornado diagram of sensitive analysis results.

511 5.6 Model validation

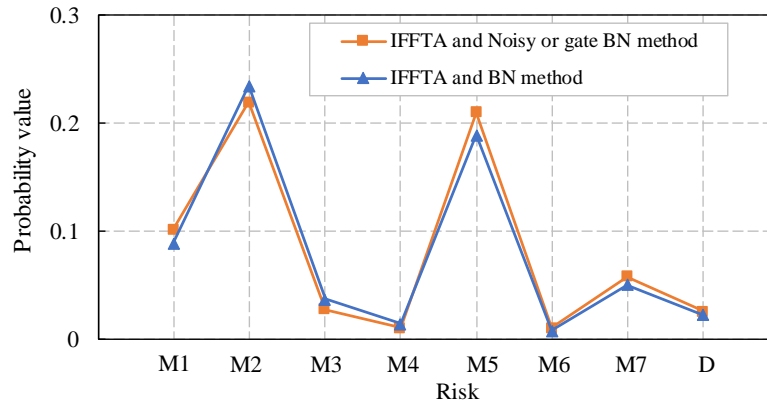
512 To verify the proposed model, the results of comparison of fuzzy failure probability between
 513 traditional FBN method and improved IFBN method are presented in Fig. 15. It is observed that the
 514 improved method generally produces smaller calculation results compared to the traditional method.
 515 This is because current approach divides the probability regions corresponding to TIFN into more
 516 reasonable intervals, leading to more accurate accident probability estimates for derailments at RTs.
 517 The traditional method was initially proposed and has been widely adopted for assessing the failure
 518 probability of human-machine systems. However, for other industries, the evaluation results are subject
 519 to inevitable objective errors. The proposed method in this study can help to mitigate the subjective
 520 understanding bias that arises when converting qualitative empirical knowledge into quantitative
 521 failure probability.



522

523 Fig. 15. Comparison of FFP of root nodes between improved IFBN and traditional method.

524 In addition, to confirm the efficacy of the Noisy or gate model, we examined the conditional
525 probabilities of each node to validate the effectiveness of the proposed model. The results of a
526 comparison between the IFFTA and Noisy or gate BN method and the IFTA and BN method are
527 presented in Fig. 16. It can be observed that there is a minimal difference between the IFFTA and Noisy
528 or gate BN model and the IFFTA and BN model. The proposed approach incorporating the Noisy or
529 gate model can not only meet the accuracy requirements for practical analysis but also reduce the
530 number of parameters necessary for BN analysis.



531
532 Fig. 16. Comparison of probability obtained by Noisy or gate IFBN method and IFBN method.

533 5.7 Preventive measures

534 By conducting a quantitative risk analysis of freight train passes through RTs, measures can be
535 taken to mitigate the risk of derailment and reduce the secondary damages and injuries caused by
536 derailed vehicles.

- 537 (1) When freight wagons pass over the vehicle retarder in front of the turnout, an intense
538 longitudinal impact will occur between the adjacent wagons. It is recommended to adjust the
539 position of the vehicle retarder in order to reduce the impact of the retarder on the operation
540 of the vehicle in the turnout area.
- 541 (2) Regular inspections and maintenance should be carried out to detect and repair any damage
542 or deviations in the geometry of turnouts in a timely manner. Due to high transportation
543 demand, various defects are more likely to occur at turnouts during operation. Railroad
544 operators should install track condition online monitoring and warning equipment in the
545 turnout area to ensure train safety and prevent secondary damages.
- 546 (3) Proper lubrication of the switch rail needs to be carried out to reduce friction, rail wear and
547 derailment coefficient. This can decrease the lateral force between the wheel and switch rail
548 and reduce the risk of wheel climb derailment.
- 549 (4) The track alignment and parameters before the turnout should be optimized. Small radius
550 curves should be avoided as much as possible from being laid in front of the turnout.

551 5 Conclusions

552 The railway turnout area is a high-risk area for freight train derailment. It is significant to quantify
553 the freight train derailment risk at turnouts and reduce the secondary damage to surrounding
554 environment, buildings, and infrastructures. This paper presents a failure probability assessment
555 method and demonstrates its application in quantifying the risk of derailment due to unfavourable
556 operating conditions in railway vehicles and turnout systems. The approach utilized in this study is
557 based on the IFFTA and NGBN model. The combination of expert elicitation, IFS, and improved SAM
558 is employed to calculate the FFP of BEs due to its capability to handle incomplete information and
559 hesitate decisions. The CPTs of the proposed IFBN model is derived using the Noisy-or gate technique
560 to overcome the limitations of complex node computation and data dependency in this study.

561 The feasibility and efficacy of risk analysis method are demonstrated by analysing the empirical
 562 data from derailment incidents in the turnout area at Taiyuan North marshalling station in China. The
 563 derailment risk at RTs can be estimated using Bayesian forward analysis and the posterior probabilities
 564 and critical events can be identified by Bayesian backward analysis. The results indicate that the
 565 derailment probability at RTs is 2.52%. Additionally, intense impact between adjacent wagons, vehicle
 566 overspeed, twist of track and severe rail are assessed as the four most influential basic factors. When
 567 compared with traditional method, the results obtained from the IFFTA and Noisy or gate BN model
 568 with improved SAM method are more reasonable when considering proper division for the linguistic
 569 terms. In this paper, the IFBN model is applied to TTS, but the same method can be potentially used
 570 to other systems for failure prediction, especially for tasks involving multiple risk sources for which
 571 accurate data are difficult to obtain.

572 The main contributions of this study can be summarized as follows: (1) An IFBN-reliability
 573 method is proposed for quantitative assessment for derailment risk at RTs. This method is capable of
 574 efficiently handling the derailment probability at RTs when prior information of the system components
 575 is incomplete and the decision environment is complex and hesitating. (2) A case study at Taiyuan
 576 North marshalling yard is presented to verify the accuracy of the proposed IFFTA and NGBN method.
 577 The comparative analysis between current method and traditional method is also carried out. The
 578 analysis results illustrate that it can meet the requirements of derailment probability assessment at RTs.
 579 (3) The critical risk factors and sensitivity analysis of the TTS are discussed, and the derailment risk at
 580 RTs can be updated by monitoring the real-time conditions of the TTS. Preventive measures for risk-
 581 based design of TTS and reducing the secondary damage caused by derailed vehicles are provided.

582 Dynamic risk assessment in the turnout area is crucial for ensuring safe and reliable railway
 583 transportation. With the continuous development of monitoring technology, we can collect more and
 584 finer monitoring data to improve the accuracy and reliability of the BN model. Besides, machine
 585 learning techniques can help us uncover potential patterns and correlations in monitoring data, thus
 586 better assessing the dynamic risk in railway switch areas. Therefore, in future work, we will apply the
 587 method of combining monitoring data and the BN model to the real-time warning system, so that the
 588 dynamic risk of derailment can be detected in advance and targeted measures can be taken to prevent
 589 accidents.

590 Declaration of Competing Interest

591 The authors declared that there is no conflict of interest.

592 Acknowledgments

593 The work was supported by the Chinese Scholarship Council (Grant No. 202207000077),
 594 National Natural Science Foundation of China (Grant No. 52122810 and 52108418), and Natural
 595 Science Foundation of Sichuan Province (Grant No. 2023NSFSC0398). The authors also thank the
 596 anonymous reviewers for their valuable comments that have improved the quality of this paper.

597 Appendix A. Derailments occurred at RTs and conditions of TTS

	Track No. alignments before turnout	Distance between retarder and turnout	Use of guard rails	Lubricat measure	Climbin g position	Falling location	Sleeper type	Loading condition	Track condition	Longitudinal slope before turnout
1	Curved line (R=200 m)	>14 m	No	Lack of lubricati on	Front zone of switch	Heel of switch	Concrete sleeper with rail brace	Empty wagon	Poor track geometry	—
2	Curved line (R=200 m)	>14 m	No	Lack of lubricati on	Front zone of switch	Heel of switch	Concrete sleeper with rail brace	Empty wagon	poor track geometry	—
3	Straight line	<14 m	Yes	Lack of lubricati on	Front zone of switch	Heel of switch	Concrete sleeper with rail brace	Empty wagon	Good track geometry	-2.6‰

4	Straight line	<14 m	Yes	Lack of lubrication	Front zone of switch	Heel of switch	Concrete sleeper with rail brace	Empty wagon	Good track geometry	-2.6‰
5	Straight line	<14 m	Yes	Lack of lubrication	Front zone of switch	Heel of switch	Concrete sleeper with rail brace	Empty wagon	Good track geometry	-4.2‰
6	Straight line	>14 m	No	Lack of lubrication	Front zone of switch	Heel of switch	Concrete sleeper with rail brace	Empty wagon	Good track geometry	-3.5‰
7	Straight line	>14 m	No	Lack of lubrication	Front zone of switch	Heel of switch	Concrete sleeper with rail brace	Empty wagon	Good track geometry	-3.5‰
8	Curved line (R=180 m)	Without vehicle retarder	Yes	Lack of lubrication	Front zone of switch	Heel of switch	Concrete sleeper with rail brace	Empty wagon	Good track geometry Poor manufacturing	—
9	Curved line (R=180 m)	Without vehicle retarder	Yes	Lack of lubrication	Front zone of switch	Heel of switch	Concrete sleeper with rail brace	Empty wagon	Good track geometry Poor manufacturing	—
10	Curved line (R=150 m)	>14 m	Yes	Lack of lubrication	Front zone of switch	Heel of switch	Concrete sleeper with rail brace	Empty wagon	Good track geometry Poor manufacturing	—

598 Appendix B Details of BEs and fuzzy failure probability

BEs	Description	Aggregated intuitionistic fuzzy number	FPS	FFP
X1	Failure of vehicle components	0.5496, 0.5849, 0.6201; 0.5403, 0.5849, 0.6295	0.5849	0.0019
X2	Intense impact between adjacent wagons	0.9088, 0.9209, 0.9330; 0.9068, 0.9209, 0.9350	0.9209	0.0572
X3	Longitudinal deviation of vehicle center of gravity	0.6557, 0.6866, 0.7175; 0.6533, 0.6866, 0.7199	0.6866	0.0042
X4	Lateral deviation of vehicle center of gravity	0.5363, 0.5732, 0.6102; 0.5264, 0.5732, 0.6200	0.5732	0.0018
X5	Train overspeed	0.9072, 0.9216, 0.9359; 0.9048, 0.9216, 0.9383	0.9216	0.0578
X6	Type of train formation: two loaded wagons sandwiched between an empty wagon	0.9441, 0.9550, 0.9659; 0.9441, 0.9550, 0.9659	0.9550	0.1118
X7	Type of train formation: three consecutive empty wagons	0.9441, 0.9550, 0.9659; 0.9441, 0.9550, 0.9659	0.9550	0.1118
X8	Type of train formation: single empty wagon	0.9029, 0.9172, 0.9315; 0.9005, 0.9172, 0.9339	0.9172	0.0536
X9	Severe wheel flange wear	0.3043, 0.3363, 0.3684; 0.2984, 0.3363, 0.3743	0.3360	0.0003
X10	Severe rail wear	0.7305, 0.7575, 0.7845; 0.7284, 0.7575, 0.7866	0.7575	0.0072
X11	Combination between new switch rail and worn stock rail	0.3810, 0.4176, 0.4543; 0.3712, 0.4176, 0.4640	0.4176	0.0005
X12	Deviation of relative height between switch and stock rail	0.8303, 0.8480, 0.8657; 0.8288, 0.8480, 0.8672	0.8480	0.0189
X13	Lateral misalignment of rail joint	0.2740, 0.3073, 0.3405; 0.2651, 0.3073, 0.3494	0.3073	0.0002
X14	Vertical misalignment of rail joint	0.1629, 0.1868, 0.2106; 0.1610, 0.1868, 0.2125	0.1868	0.0001
X15	Manufacturing defects	0.1609, 0.1890, 0.2171; 0.1586, 0.1890, 0.2194	0.1890	0.0001
X16	Broken rails	0.0513, 0.0654, 0.0779; 0.0504, 0.0654, 0.0788	0.0649	0.0000
X17	Buckled rails	0.0928, 0.1096, 0.1244; 0.0917, 0.1096, 0.1255	0.1089	0.0000
X18	Short straight line before RT	0.9441, 0.9550, 0.9659; 0.9441, 0.9550, 0.9659	0.9550	0.1118

X19	Sharp curve line before RT	0.9441, 0.9550, 0.9659; 0.9441, 0.9550, 0.9659	0.9550	0.1118
X20	Large longitudinal slope before RT	0.9030, 0.9175, 0.9319; 0.9006, 0.9175, 0.9343	0.9175	0.0539
X21	Inappropriate super elevation	0.9135, 0.9253, 0.9371; 0.9115, 0.9253, 0.9390	0.9253	0.0618
X22	Wooden sleepers replaced by concrete sleepers	0.1246, 0.1440, 0.1612; 0.1233, 0.1440, 0.1625	0.1433	0.0001
X23	Use of rail brace	0.1545, 0.1764, 0.1983; 0.1528, 0.1764, 0.2000	0.1764	0.0001
X24	Lack of lubrication for rails	0.9030, 0.9175, 0.9319; 0.9006, 0.9175, 0.9343	0.9175	0.0539
X25	Rail gauge deviation	0.3916, 0.4267, 0.4618; 0.3822, 0.4267, 0.4712	0.4267	0.0006
X26	Rail height deviation	0.4638, 0.5000, 0.5362; 0.4541, 0.5000, 0.5459	0.5000	0.0010
X27	Existing gap between stock rail and switch rail	0.1548, 0.1772, 0.1996; 0.1530, 0.1772, 0.2013	0.1772	0.0001
X28	Rail support failure	0.1914, 0.2170, 0.2425; 0.1893, 0.2170, 0.2446	0.2170	0.0001

599 References

- 600 [1] S.W. Kirkpatrick, C.-Y. Lin, L. Iannacone, P. Gharzouzi, T. Treichel, C.P. Barkan, P.
601 Gardoni, Derailment Analysis for Prediction of Damage and Probability of Release for Novel
602 Railroad Tank Car Designs, *Transportation Research Record*, (2022) 03611981221137589.
603 [2] C.-Y. Lin, M. Rapik Saat, C.P. Barkan, Quantitative causal analysis of mainline passenger
604 train accidents in the United States, *Proceedings of the Institution of Mechanical Engineers*,
605 Part F: *Journal of Rail and Rapid Transit*, 234 (2020) 869-884.
606 [3] S. Dindar, S. Kaewunruen, Assessment of turnout-related derailments by various causes,
607 in: *Recent Developments in Railway Track and Transportation Engineering: Proceedings of*
608 *the 1st GeoMEast International Congress and Exhibition, Egypt 2017 on Sustainable Civil*
609 *Infrastructures 1*, Springer, 2018, pp. 27-39.
610 [4] X. Liu, M.R. Saat, C.P. Barkan, Analysis of causes of major train derailment and their
611 effect on accident rates, *Transportation Research Record*, 2289 (2012) 154-163.
612 [5] J. Lai, J. Xu, P. Wang, Z. Yan, S. Wang, R. Chen, J. Sun, Numerical investigation of
613 dynamic derailment behavior of railway vehicle when passing through a turnout, *Engineering*
614 *Failure Analysis*, 121 (2021) 105132.
615 [6] X. Wu, M. Chi, H. Gao, Post-derailment dynamic behaviour of a high-speed train under
616 earthquake excitations, *Engineering Failure Analysis*, 64 (2016) 97-110.
617 [7] S. Kaewunruen, Y. Wang, C. Ngamkhanong, Derailment-resistant performance of modular
618 composite rail track slabs, *Engineering Structures*, 160 (2018) 1-11.
619 [8] W. Huang, Y. Zhang, B. Zuo, Y. Yu, G.J. De Dieu, Y. Xu, Using an expanded Safety Failure
620 Event Network to analyze railway dangerous goods transportation system risk-accident,
621 *Journal of Loss Prevention in the Process Industries*, 65 (2020) 104122.
622 [9] P. Wang, *Design of high-speed railway turnouts: theory and applications*, Academic Press,
623 2015.
624 [10] X. Liu, Statistical temporal analysis of freight train derailment rates in the United States:
625 2000 to 2012, *Transportation research record*, 2476 (2015) 119-125.
626 [11] J. Lai, J. Xu, T. Liao, Z. Zheng, J. Chen, S. Wang, P. Wang, Effect of lateral misalignment
627 defects of rail joints on dynamic derailment behaviour in railway turnouts, *Vehicle System*
628 *Dynamics*, (2022) 1-22.
629 [12] M. Durali, M. Jalili, A new criterion for assessment of train derailment risk, *Proceedings*

630 of the Institution of Mechanical Engineers, Part K: Journal of Multi-body Dynamics, 224
631 (2010) 83-101.

632 [13] X. Ge, L. Ling, L. Guo, Z. Shi, K. Wang, Dynamic derailment simulation of an empty
633 wagon passing a turnout in the through route, *Vehicle System Dynamics*, 60 (2022) 1148-1169.

634 [14] N. Burgelman, Z. Li, R. Dollevoet, Fast estimation of the derailment risk of a braking
635 train in curves and turnouts, *International journal of heavy vehicle systems*, 23 (2016) 213-
636 229.

637 [15] J. Lai, J. Xu, T. Liao, Z. Zheng, R. Chen, P. Wang, Investigation on train dynamic
638 derailment in railway turnouts caused by track failure, *Engineering Failure Analysis*, 134
639 (2022) 106050.

640 [16] J. Lai, J. Xu, Z. Zheng, P. Wang, S. Wang, Influence of the motion conditions of wheelsets
641 on dynamic derailment behaviour of a bogie in railway turnouts, *Vehicle System Dynamics*,
642 60 (2022) 3720-3742.

643 [17] E. Ruijters, M. Stoelinga, Fault tree analysis: A survey of the state-of-the-art in modeling,
644 analysis and tools, *Computer science review*, 15 (2015) 29-62.

645 [18] R. Ferdous, F. Khan, R. Sadiq, P. Amyotte, B. Veitch, Handling data uncertainties in event
646 tree analysis, *Process safety and environmental protection*, 87 (2009) 283-292.

647 [19] P. Bhattacharjee, V. Dey, U. Mandal, Risk assessment by failure mode and effects analysis
648 (FMEA) using an interval number based logistic regression model, *Safety Science*, 132 (2020)
649 104967.

650 [20] W.-K. Ching, M.K. Ng, Markov chains, Models, algorithms and applications, (2006).

651 [21] P. Trucco, E. Cagno, F. Ruggeri, O. Grande, A Bayesian Belief Network modelling of
652 organisational factors in risk analysis: A case study in maritime transportation, *Reliability
653 Engineering & System Safety*, 93 (2008) 845-856.

654 [22] J.L. Peterson, Petri nets, *ACM Computing Surveys (CSUR)*, 9 (1977) 223-252.

655 [23] S. Kabir, An overview of fault tree analysis and its application in model based
656 dependability analysis, *Expert Systems with Applications*, 77 (2017) 114-135.

657 [24] T.H.A. Nguyen, J. Trinckauf, T.A. Luong, T.T. Truong, Risk analysis for train collisions
658 using fault tree analysis: case study of the Hanoi urban mass rapid transit, *Urban Rail Transit*,
659 8 (2022) 246-266.

660 [25] W. Huang, Y. Liu, Y. Zhang, R. Zhang, M. Xu, G.J. De Dieu, E. Antwi, B. Shuai, Fault
661 Tree and Fuzzy DS Evidential Reasoning combined approach: An application in railway
662 dangerous goods transportation system accident analysis, *Information Sciences*, 520 (2020)
663 117-129.

664 [26] E. Jafarian, M. Rezvani, Application of fuzzy fault tree analysis for evaluation of railway
665 safety risks: an evaluation of root causes for passenger train derailment, *Proceedings of the
666 Institution of Mechanical Engineers, Part F: Journal of Rail and Rapid Transit*, 226 (2012) 14-
667 25.

668 [27] C.-Y. Lin, M.R. Saat, C.P. Barkan, Fault tree analysis of adjacent track accidents on
669 shared-use rail corridors, *Transportation Research Record*, 2546 (2016) 129-136.

670 [28] N. Esmaeeli, F. Sattari, L. Lefsrud, R. Macciotta, Assessing the Risks Associated with the
671 Canadian Railway System Using a Safety Risk Model Approach, *Transportation Research
672 Record*, (2023) 03611981231176549.

673 [29] L.A. Zadeh, Fuzzy sets, *Information and control*, 8 (1965) 338-353.

674 [30] J.A.D. Santana, J.L. Orozco, D. Furka, S. Furka, Y.C.B. Matos, D.F. Lantigua, A.G.
675 Miranda, M.C.B. González, A new Fuzzy-Bayesian approach for the determination of failure
676 probability due to thermal radiation in domino effect accidents, *Engineering Failure Analysis*,
677 120 (2021) 105106.

678 [31] A. Chelilyan, S. Bhattacharyya, Fuzzy fault tree analysis of oil and gas leakage in subsea
679 production systems, *Journal of Ocean Engineering and Science*, 3 (2018) 38-48.

680 [32] K.T. Atanassov, Intuitionistic fuzzy sets, *Fuzzy Sets and Systems*, 20 (1986) 87-96.

681 [33] H. Garg, A novel approach for analyzing the behavior of industrial systems using weakest
682 t-norm and intuitionistic fuzzy set theory, *ISA transactions*, 53 (2014) 1199-1208.

683 [34] M. Kaushik, M. Kumar, An integrated approach of intuitionistic fuzzy fault tree and
684 Bayesian network analysis applicable to risk analysis of ship mooring operations, *Ocean
685 Engineering*, 269 (2023) 113411.

686 [35] J. Yu, Q. Zeng, Y. Yu, S. Wu, H. Ding, H. Gao, J. Yang, An intuitionistic fuzzy
687 probabilistic Petri net method for risk assessment on submarine pipeline leakage failure,
688 *Ocean Engineering*, 266 (2022) 112788.

689 [36] M. Kumar, M. Kaushik, System failure probability evaluation using fault tree analysis
690 and expert opinions in intuitionistic fuzzy environment, *Journal of loss prevention in the
691 process industries*, 67 (2020) 104236.

692 [37] Q. Yu, Â.P. Teixeira, K. Liu, H. Rong, C.G. Soares, An integrated dynamic ship risk model
693 based on Bayesian Networks and Evidential Reasoning, *Reliability Engineering & System
694 Safety*, 216 (2021) 107993.

695 [38] Y. Jianxing, W. Shibo, Y. Yang, C. Haicheng, F. Haizhao, L. Jiahao, G. Shenwei, Process
696 system failure evaluation method based on a Noisy-OR gate intuitionistic fuzzy Bayesian
697 network in an uncertain environment, *Process Safety and Environmental Protection*, 150 (2021)
698 281-297.

699 [39] Z. Li, S. Hu, G. Gao, C. Yao, S. Fu, Y. Xi, Decision-making on process risk of Arctic
700 route for LNG carrier via dynamic Bayesian network modeling, *Journal of Loss Prevention in
701 the Process Industries*, 71 (2021) 104473.

702 [40] C.E. Kahn Jr, L.M. Roberts, K.A. Shaffer, P. Haddawy, Construction of a Bayesian
703 network for mammographic diagnosis of breast cancer, *Computers in biology and medicine*,
704 27 (1997) 19-29.

705 [41] P. Gehl, D. D'ayala, Development of Bayesian Networks for the multi-hazard fragility
706 assessment of bridge systems, *Structural Safety*, 60 (2016) 37-46.

707 [42] X. Lei, Y. Xia, Y. Dong, L. Sun, Multi-level time-variant vulnerability assessment of
708 deteriorating bridge networks with structural condition records, *Engineering Structures*, 266
709 (2022) 114581.

710 [43] Y. Tang, S. Huang, Assessing seismic vulnerability of urban road networks by a Bayesian
711 network approach, *Transportation research part D: transport and environment*, 77 (2019) 390-
712 402.

713 [44] S. Dindar, S. Kaewunruen, M. An, J.M. Sussman, Bayesian Network-based probability
714 analysis of train derailments caused by various extreme weather patterns on railway turnouts,
715 *Safety science*, 110 (2018) 20-30.

716 [45] C. Ji, X. Su, Z. Qin, A. Nawaz, Probability analysis of construction risk based on noisy-
717 or gate bayesian networks, *Reliability Engineering & System Safety*, 217 (2022) 107974.

718 [46] V. Cozzani, S. Bonvicini, G. Spadoni, S. Zanelli, Hazmat transport: A methodological
719 framework for the risk analysis of marshalling yards, *Journal of Hazardous Materials*, 147
720 (2007) 412-423.

721 [47] Z. Jianping, L. Pide, Z. Qiang, G. Shuai, Practice on operation safety quality control of
722 marshalling yard, *China Safety Science Journal*, 28 (2018) 60.

723 [48] Y. Ye, J. Zhang, H. Liang, An acoustic-based recognition algorithm for the unreleased
724 braking of railway wagons in marshalling yards, *IEEE Access*, 8 (2020) 120295-120308.

725 [49] J. Lai, J. Xu, Y. Chen, Z. Zheng, J. Wang, P. Wang, Evaluation of dynamic derailment in
726 a railway switch considering the longitudinal impacts caused by vehicle retarder, *Proceedings
727 of the Institution of Mechanical Engineers, Part F: Journal of Rail and Rapid Transit*, 237
728 (2023) 806-817.

729 [50] H.-L. Chang, L.-S. Ju, Effect of consecutive driving on accident risk: a comparison
730 between passenger and freight train driving, *Accident Analysis & Prevention*, 40 (2008) 1844-
731 1849.

732 [51] X. Liu, Optimizing rail defect inspection frequency to reduce the risk of hazardous
733 materials transportation by rail, *Journal of Loss Prevention in the Process Industries*, 48 (2017)
734 151-161.

735 [52] X. Wang, X. Liu, Z. Bian, A machine learning based methodology for broken rail
736 prediction on freight railroads: A case study in the United States, *Construction and Building
737 Materials*, 346 (2022) 128353.

738 [53] M.F. Ishak, S. Dindar, S. Kaewunruen, Safety-based maintenance for geometry
739 restoration of railway turnout systems in various operational environments, in: *Proceedings
740 of The 21st National Convention on Civil Engineering, Songkhla THAILAND*, 2016.

741 [54] S. Dindar, S. Kaewunruen, M. An, Bayesian network-based human error reliability
742 assessment of derailments, *Reliability Engineering & System Safety*, 197 (2020) 106825.

743 [55] P. Liu, L. Yang, Z. Gao, S. Li, Y. Gao, Fault tree analysis combined with quantitative
744 analysis for high-speed railway accidents, *Safety science*, 79 (2015) 344-357.

745 [56] G. Wang, T. Xu, T. Tang, T. Yuan, H. Wang, A Bayesian network model for prediction of
746 weather-related failures in railway turnout systems, *Expert systems with applications*, 69
747 (2017) 247-256.

748 [57] C. Liang, M. Ghazel, O. Cazier, L. Bouillaut, Advanced model-based risk reasoning on
749 automatic railway level crossings, *Safety science*, 124 (2020) 104592.

750 [58] E. Castillo, A. Calviño, Z. Grande, S. Sánchez - Cambronero, I. Gallego, A. Rivas, J.M.
751 Menéndez, A Markovian - Bayesian network for risk analysis of high speed and conventional
752 railway lines integrating human errors, *Computer - Aided Civil and Infrastructure
753 Engineering*, 31 (2016) 193-218.

754 [59] W. Huang, Y. Zhang, X. Kou, D. Yin, R. Mi, L. Li, Railway dangerous goods
755 transportation system risk analysis: An Interpretive Structural Modeling and Bayesian
756 Network combining approach, *Reliability Engineering & System Safety*, 204 (2020) 107220.

757 [60] P. Rungskunroch, A. Jack, S. Kaewunruen, Benchmarking on railway safety performance
758 using Bayesian inference, decision tree and petri-net techniques based on long-term accidental

759 data sets, *Reliability Engineering & System Safety*, 213 (2021) 107684.
760 [61] J. Zeng, P. Wu, Study on the wheel/rail interaction and derailment safety, *Wear*, 265 (2008)
761 1452-1459.
762 [62] J. Dunj3, V. Fthenakis, J.A. V3lchez, J. Arnaldos, Hazard and operability (HAZOP)
763 analysis. A literature review, *Journal of hazardous materials*, 173 (2010) 19-32.
764 [63] D.H. Stamatis, *Failure mode and effect analysis: FMEA from theory to execution*, Quality
765 Press, 2003.
766 [64] S. Dindar, S. Kaewunruen, M. An, Identification of appropriate risk analysis techniques
767 for railway turnout systems, *Journal of Risk Research*, 21 (2018) 974-995.
768 [65] H.-M. Hsu, C.-T. Chen, Aggregation of fuzzy opinions under group decision making,
769 *Fuzzy sets and systems*, 79 (1996) 279-285.
770 [66] M. Yazdi, S. Kabir, Fuzzy evidence theory and Bayesian networks for process systems
771 risk analysis, *Human and Ecological Risk Assessment: An International Journal*, 26 (2020)
772 57-86.
773 [67] D.H. Hong, H.Y. Do, Fuzzy system reliability analysis by the use of T_{ω} (the weakest t-
774 norm) on fuzzy number arithmetic operations, *Fuzzy Sets and Systems*, 90 (1997) 307-316.
775 [68] A. Varghese, R.R. Varghese, K. Balakrishnan, J.S. Paul, Level identification of brain MR
776 images using histogram of a LBP variant, in: *2012 IEEE International Conference on*
777 *Computational Intelligence and Computing Research*, IEEE, 2012, pp. 1-4.
778 [69] T. Onisawa, A representation of human reliability using fuzzy concepts, *Information*
779 *Sciences*, 45 (1988) 153-173.
780 [70] F.V. Jensen, T.D. Nielsen, *Bayesian networks and decision graphs*, Springer, 2007.
781 [71] X. Feng, J.-c. Jiang, W.-f. Wang, Gas pipeline failure evaluation method based on a Noisy-
782 OR gate bayesian network, *Journal of Loss Prevention in the Process Industries*, 66 (2020)
783 104175.
784